Influence of the Molecular Structure of Polyolefins on the Damping Function in Shear

Florian J. Stadler,[†] Dietmar Auhl,[‡] and Helmut Münstedt*

Institute of Polymer Materials, Friedrich-Alexander-University Erlangen-Nürnberg, Martensstr. 7, 91058 Erlangen, Germany

Received August 6, 2007; Revised Manuscript Received February 5, 2008

ABSTRACT: This paper deals with the nonlinear shear behavior of linear and long-chain branched polyethylenes (PE) and polypropylenes (PP) as determined at high step strains. For linear polyethylenes, the comonomer content, molar mass, and molar mass distribution were confirmed to have no influence on the damping function, while a clear difference between linear PP and PE was obvious. Long-chain branched metallocene catalyzed polyethylene (mPE) as well as irradiated long-chain branched PP samples showed a weaker strain dependence compared to their linear counterparts depending on the amount of branching. With an increasing number of long-chain branches, this trend becomes more pronounced. Most of the damping functions measured can well be described by a function similar to the Carreau−Yasuda equation. The relation of the three parameters of this equation with the molecular structure of the samples is discussed.

Introduction

Step shear experiments are widely used for polymer melts to determine the strain dependence of the relaxation modulus.

$$G(t, \gamma_0) = \tau(t, \gamma_0)/\gamma_0 \tag{1}$$

with (τ, γ_0) being the time-dependent shear stress following the shear step. In many cases, the time and strain dependence of the modulus $G(t, \gamma_0)$ has been found to be separable according to

$$G(t, \gamma_0) = G^0(t)\, h(\gamma_0) \tag{2}$$

$G^0(t)$ describes the time-dependent modulus in the linear range and $h(\gamma_0)$ the so-called damping function. The validity of the separability was verified, for example, for a long-chain branched polyethylene by Wagner and Laun,[1] for polydimethylsiloxanes by Papanastasiou et al.,[2] and for polyethylenes and polystyrenes by Soskey and Winter.[3]

For a particular linear polymer melt, the damping function is independent of molar mass[4] and temperature.[1,4−6] Polydispersity can change $h(\gamma_0)$, as was shown in literature.[7−9] For polypropylenes with polydispersities between 2.8 and 5.6, no influence of the molar mass and its distribution width was found, however.[10]

Furthermore, the chemical structure of a polymer affects $h(\gamma_0)$. The difference of the shear damping functions of commercial linear polyethylene and polypropylene with broad molar mass distributions has been shown.[11] For long-chain branched polymers, it is well-known that they possess a significantly smaller strain dependence.[11−13] However, it has been reported that branched polymers consisting of only three-arm and four-arm stars do not show any sizable difference to the nonlinear behavior of linear polymers (only a weak tendency toward a more pronounced deformation dependence is observed).[14−16]

For pom-pom-shaped molecules with three arms on each side, the time−strain separability is not given, but a time-dependent damping function is found (which means that a true damping function does not exist).[17] Hepperle and Münstedt[6] found no influence of the topography on the time−strain separability for polystyrene combs but confirm the reduction of the strain dependence by the introduction of long-chain branches. This finding was recently affirmed by Kirkwood et al. for polyisoprene combs.[18]

The reasons for the different dependencies of the relaxation behavior on molecular structures are still not yet fully understood. The nonlinearity of the relaxation modulus is regarded to originate from the induced chain anisotropy and the decrease in entanglement density induced by the large shear amplitude. For branched polymers, the hindered relaxation of a chain segment, which is constrained by two branch points (no reptation), is considered as a very probable explanation for the weaker strain dependence of the damping function.[5] A theoretical explanation is given elsewhere.[19,20]

The relaxation behavior after the step strain can be used for the comparison of predictions of different models and theories. In the case of a relaxation experiment, for example, the tube reptation theory of Doi and Edwards (DE) predicts not only the linear but also the nonlinear-viscoelastic behavior.[21] The DE-damping function with independent alignment can be expressed by eq 3[22] with $\alpha = 5$ and $\beta = 2$:[6,16,19,23]

$$h(\gamma_0) = \frac{\alpha}{\alpha + {\gamma_0}^{\beta}} \tag{3}$$

A physical meaning of the coefficients α and β is not given, however. A good agreement of this formula was found with experimental data of narrowly distributed linear samples and in some cases stars.[6,15,16,18] However, eq 3 does not well describe polymer melts with broad molar mass distributions and long-chain branching.

Soskey and Winter[3,24] proposed a different form of the same equation, but in their case, the parameters α $(= 1/a)$ and β $(= b)$ were set to be freely adjustable fitting parameters. In the DE-[22] and the PSM-model,[2] α and β are fixed (DE, $\alpha = 5$ $\beta = 2$; PSM, $\alpha = 7.8$ $\beta = 2$).

Other different forms of damping functions were proposed in the past for the description of the experimental shear damping functions, e.g., Papanastasiou−Scriven−Macosko (PSM),[2]

* To whom correspondence should be addressed. E-mail: helmut.muenstedt@ww.uni-erlangen.de. Phone: +49 9131 852 7604. Fax: +49 9131 852 8321.

[†] Current address: Unité de Physique et de Chimie des Hauts Polymères, Université Catholique de Louvain, Croix du Sud, 1, B-1348 Louvain-la-Neuve, Belgium.

[‡] Current address: Interdisciplinary Research Centre (IRC) in Polymer Science and Technology University of Leeds, LS2 9JT Leeds, United Kingdom (GB).

10.1021/ma0717587 CCC: $40.75
Published on Web 04/22/2008

Table 1. Molecular Data of the Polyethylenes

sample	long-chain branching	M_w (kg/mol)	M_w/M_n
L8	none	86	2
C2	none	114	16
C3	none	120	2
ZN-HDPE	none	124	4
F26C	none	175	2
D4	very low[a]	74	2
B5	low[a]	61	2
B10	low[a]	65	2
B9	medium	65	2
LDPE 5	high	158	14

[a] No branches were detected by SEC-MALLS for these samples, but rheological measurements in the linear-viscoelastic regime and the temperature dependence clearly indicate that the samples are long-chain branched.[28,30]

Table 2. Molecular Data of the Polypropylenes

sample	long-chain branching	M_w (kg/mol)	M_w/M_n
PP-A	none	669	4
PP-B	none	452	6
PP-C	none	406	2
mPP-C	none	345	3
PP-B2	very low[a]	347	5
PP-B10	low	304	4
PP-B20	low	262	4
PP-B60	medium	213	4
PP-B100	high	210	4

[a] No branches were detected by SEC-MALLS for this sample, but rheological measurements in the linear-viscoelastic regime clearly indicate that the sample is long-chain branched.[37]

Wagner−Demarmels (WD),[25] and Luo−Tanner (LT). Together with constitutive equations, the nonlinear relaxation behavior can be used for correlations and predictions of the rheological behavior. A strong connection was shown in the literature, e.g., between the strain-dependent behavior and transient shear flow or shear thinning of low density polyethylene (LDPE).[26]

This paper focuses on correlations between the molecular structure and the damping function. For this purpose, different linear and long-chain branched samples are characterized by relaxation tests, whose molecular structure, linear-viscoelastic response, and in some cases elongational behavior is already well-known.

The linear response and molecular data of the polyethylenes can be found in several papers elsewhere.[27–36] The shear and elongational data along with the molecular characterization of the linear and long-chain branched polypropylenes can be found in several papers elsewhere.[37–39]

Experimental Section

Materials. The samples were characterized by high temperature size exclusion chromatography with coupled multiangle laser light scattering (SEC-MALLS) operated at 140 °C with 1,2,4-TCB (trichlorobenzene) as solvent. Its setup is described by Stadler et al.[29] in detail.

The molecular data of the polyethylenes used are given in Table 1. The synthesis conditions of F26C are given by Kaminsky et al.[40] The polymerization conditions of the long-chain branched metallocene catalyzed polyethylenes (LCB-mHDPE) are published in previous papers (D4, B5, B10, B9).[30,41] ZN-HDPE is a commercial Ziegler–Natta catalyzed HDPE grade from the Basell company. F26C contains 2.3 mol % hexacosene, which is equivalent to 23.4 wt %, and L8 contains approximately 1 mol % octene, which is equivalent to ≈3.9 wt %.[31,33] All other polymers do not contain comonomers, but LDPE 5 contains side chains because of the high pressure synthesis.

The linear polypropylenes are commercial homopolymer resins. The long-chain branched polypropylenes were prepared by electron-beam irradiation from the linear precursor PP-B. Experimental details of this process and of the SEC-MALLS measurements are given in more detail elsewhere.[38] The number in the sample name indicates the irradiation dose in kGy. The precursor PP-B has a lower mass-average molar mass M_w than the polypropylene PP-A, which was used for another series of long-chain branched samples described in an earlier study.[38]

Step-Strain Tests. The sample preparation was carried out in the same way as described before.[29,38] The laboratory scale samples, C2 and L8, were stabilized with 0.5 wt % Irgafos 168 and 0.5 wt % Irganox 1010 (Ciba SC). All tests were performed on a Bohlin CVOR "Gemini" stress-controlled rotational rheometer. For the polyethylene samples, the test temperature was chosen to be 150 °C, while 180 °C was used for the polypropylene samples.

The imposition time of the strain step γ_0 was about 20 ms due to the instrument inertia for small deformations ($\gamma_0 < 300\%$), which increases to up to 1 s for the largest γ_0 (depending on the material, the maximum strain obtainable was between 700 and 10 000%). A 25 mm parallel-plate geometry was used for all tests, making a correction for large strains necessary because of the nonhomogenous flow field (the strain amplitude varies as a function of the radius). By using a parallel-plate geometry, the magnitude of the strain can be increased, while the sensitivity to gap errors can be reduced.

The choice of a stress-controlled rheometer instead of a strain-controlled one, which would be the obvious choice for stress relaxation experiments was based on several criteria. One has to consider that stress relaxation by definition imposes a high strain in a very short period of time and thus leads to high forces, which might damage a rheometer. A stress-controlled rheometer handles the imposition of the step by performing a "creep test" with the maximum stress acting until the desired deformation is reached. Another advantage is that in a stress-controlled rheometer the strain obtainable is only limited by the sample response and by the maximum force, which can be applied, while in the strain-controlled Rheometric Scientific/TA ARES the deformation in step shear is limited to a rotation of 90°, which corresponds to several 100% of strain at a gap of around 1.5 mm.

Also, one has to consider that there is basically no difference in the test profile between the strain- and stress-controlled rheometer, as the step strain applied by both rheometer types has basically the same profile. It was also tested that the step time has no relevant influence on the relaxation modulus after times longer than tenfold the maximum tested step time. Hence, the response (relaxation modulus) from stress- and strain-controlled rheometers are comparable.

A sequence of a number of relaxation tests on one sample was applied. The experiment was started with the lowest deformation, and when the stress was completely relaxed at the end of the first test, the next one with a higher deformation was started. The maximum deformation γ_0 applied was around 10 000%.

These consecutive relaxation tests can only be performed under three conditions. The first is that the remaining stress after relaxation has to be negligibly small compared to the stress applied in the next step.

The second condition is that the sample must not suffer any structural damage or degradation.

Another condition is that during the test, adhesion to the plates has to be given and that any rupture within the samples has to be avoided. This condition is hard to prove directly, as it would require rather complicated optical measurements. Indirect evidence of adhesion is given by the fact that any rupture would change the shape of the relaxation modulus $G(t)$, thus making the determination of the time-independent damping function $h(\gamma_0)$ impossible.

Determination of the Damping Function. The curves $\log G(t, \gamma_0)$ as a function of $\log t$ are found to have the same shape, indicating that the damping functions are time-independent, as it should be if the time−strain separation is valid (cf. Figure 1). Therefore, the damping functions can be calculated according to eq 2.

Because the deformation of a sample in a parallel-plate geometry is not locally constant, a correction has been made according to Soskey and Winter.[3] The apparent relaxation modulus G_{app} is corrected by a term calculated from the double-logarithmic derivative of the apparent relaxation modulus with respect to the deformations according to

$$G(t,\gamma_0) = G_{app}(t,\gamma_0)\left(1+\frac{1}{4}\frac{\mathrm{d\ lg}\ G_{app}(t,\gamma_0)}{\mathrm{d\ lg}\ \gamma_0}\right) \tag{4}$$

or following from that

$$h(\gamma_0) = h_{app}(\gamma_0)\left(1+\frac{1}{4}\frac{\mathrm{d\ lg}\ h_{app}(\gamma_0)}{\mathrm{d\ lg}\ \gamma_0}\right) \tag{5}$$

Results and Discussion

The relaxation moduli of PP-B at different deformation steps are shown in Figure 1. In good approximation, the shape of the functions obtained is the same; thus, a time-independent damping function can be determined. Frequency sweeps before and after the test show no difference. Thus, no thermal and mechanical degradation or structural damage was found.

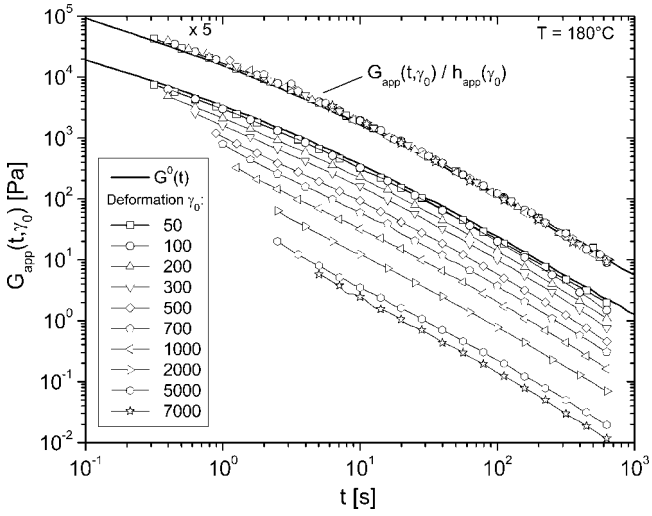

Figure 1. Example of a step shear test: apparent relaxation modulus $G_{app}(t)$ of PP-B at different deformation steps γ_0 (γ_0 is given in %). The upper curve show the moduli shifted onto the linear-viscoelastic curve. This curve is multiplied by a factor of 5 for better clarity.

Numerical Description of the Damping Functions. Different types of damping functions, i.e., Doi and Edwards (DE) and Papanastasiou−Scriven−Macosko (PSM), were examined to find the best description of the experimental shear damping functions. None of these models predict well enough all of the experimental data obtained on the large number of different samples. This is discussed later in detail for linear samples. In addition, they are not able to describe the effect of long-chain branching on the damping function (cf. Figures 5 and 7). Therefore, a numerical description covering a wide range of molecular architectures was developed.

This description is based on the observation that the shape of the damping functions in a double-logarithmic scaling is similar to that of viscosity functions (cf. Figure 2). Thus, the damping functions were modeled using a type of equation similar to that used by Carreau and Yasuda[42,43] for viscosity functions, i.e.,

$$h(\gamma_0) = \left[1+\left(\frac{\gamma_0}{\gamma_c}\right)^b\right]^{(m/b)} \tag{6}$$

Compared with the equation used for the description of viscosity functions, this form contains only three parameters, as for obvious reasons the zero shear-rate viscosity η_0 is replaced by 1. The parameters are schematically represented in Figure 2. The critical deformation γ_c is the deformation at which the tangent of $h(\gamma_0)$ for very high deformations reaches a value of 1. The parameter m is the slope of that tangent in a double-logarithmic plot, and b is the parameter representing the width of the transition between the linear-viscoelastic and the nonlinear regime.

The functions of the different models based on eq 3 have the same shape as those based on eq 6. The parameters of those models are connected to each other by the following relations:

$$m = -\beta, \quad b = \beta, \quad \text{and} \quad \gamma_c = \alpha^{1/\beta} \tag{7}$$

In comparison to eq 3, eq 6 provides the extra degree of freedom that the width of the transition zone b and the slope of the nonlinear regime m are independent of each other. This is important when measuring in the pronounced nonlinear regime, as both constants can be determined individually. Besides the independent determination of the parameters m and b, eq 6 has the advantage that the physical meaning of the critical deformation γ_c is much more obvious than that of the parameter α in the DE, PSM, or Soskey−Winter model (as mentioned before, the real DE model is derived from the DE theory and the DE model is only an approximation of the real more complicated function). This might be the reason why Soskey and Winter[3] did not discuss any physical meaning of their parameters α and β that they used for fitting.[44]

The double-logarithmic slope of eq 6 is given by

$$\frac{\mathrm{d\ lg}\ h(\gamma_0)}{\mathrm{d\ lg}\ \gamma_0} = \frac{m\left(\frac{\gamma_0}{\gamma_c}\right)^b}{1+\left(\frac{\gamma_0}{\gamma_c}\right)^b} \tag{8}$$

This equation provides another physical interpretation of γ_c, which corresponds to the deformation γ_0, where the double-logarithmic slope of the damping function reaches a value of $m/2$.

The double-logarithmic slope m is the other quantity with a physical meaning. It is the limiting slope for very high deformations.

The relevance of eq 8 lies in the need for the correction of damping functions measured by parallel-plate geometries. This correction can be performed with the fit parameters of an apparent damping function $h_{app}(\gamma_0)$ fitted with eq 5. The double-logarithmic derivative in eq 5 can then be substituted by eq 8, thus obtaining eq 9

$$h(\gamma_0) = h_{app}(\gamma_0)\left(1+\frac{1}{4}\frac{m_{app}\left(\frac{\gamma_0}{\gamma_{c,app}}\right)^{b_{app}}}{1+\left(\frac{\gamma_0}{\gamma_{c,app}}\right)^{b_{app}}}\right) \tag{9}$$

An example of the correction is shown in Figure 2. It is obvious that it changes the shape of $h(\gamma_0)$ significantly. The advantage of the correction using eq 9 is that a rather simple model is able to describe the damping function with great accuracy and that the double-logarithmic slope can be determined using an analytical expression.

The slope of the apparent damping function $h_{app}(\gamma_0)$ was found to be −1.50, while the corrected damping function $h(\gamma_0)$, using eq 8, has a slightly steeper slope of −1.51. The value of b increases slightly (2.03 apparent, 2.06 corrected). A much larger difference, however, can be observed for the value of γ_c with 197 and 158%, respectively. As the shape of all damping functions is very similar, these differences are representative.

Damping Functions of Linear Samples. The tests on the linear PE and PP samples were carried out to determine the

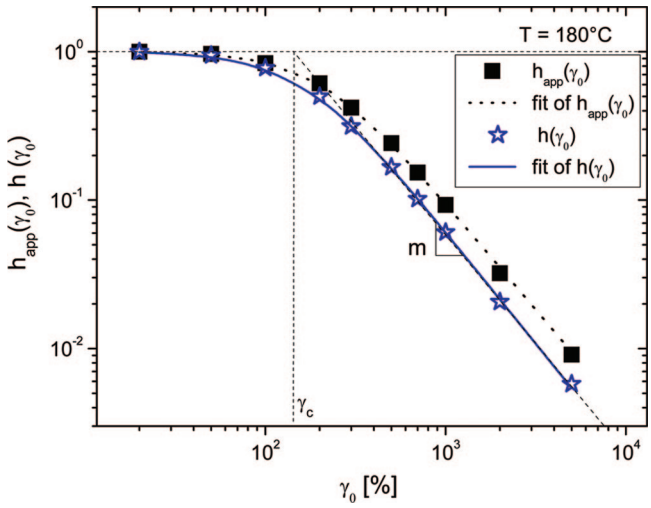

Figure 2. Example for the correction of the damping function of PP-B.

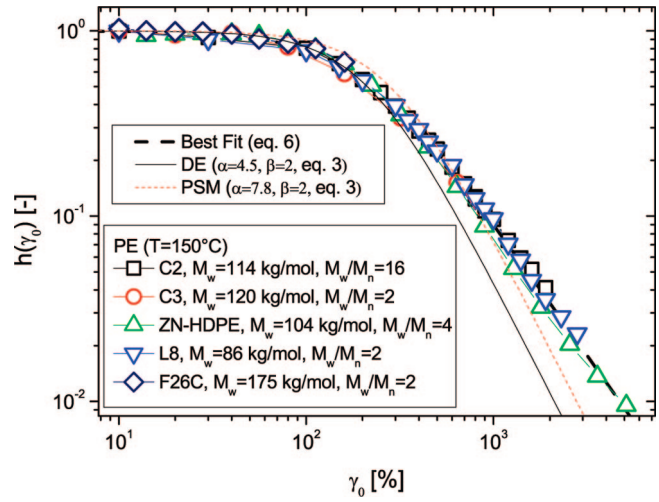

Figure 3. Damping functions of the linear PE and their numerical descriptions.

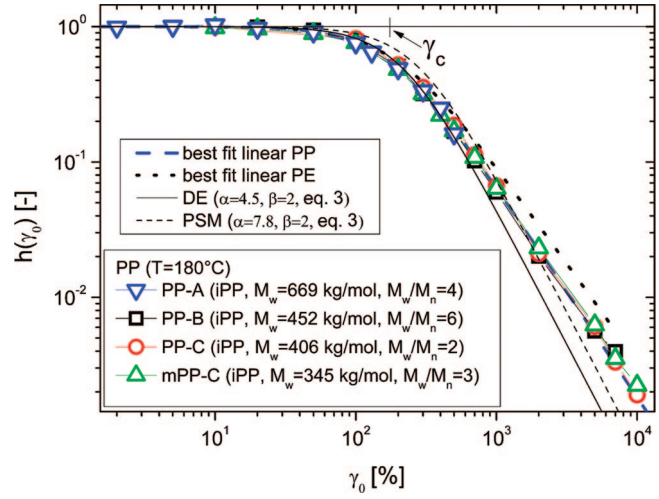

Figure 4. Damping functions of the linear PP and their numerical descriptions.

influence of molar mass M_w, molar mass distribution, comonomer content, and type of polymer on the damping function.

Polyethylenes. The damping functions of the five linear polyethylenes are shown in Figure 3 These damping functions are very similar in shape. Therefore, it can be concluded from Figure 3 that the molar mass distribution and the comonomer content (L8: $n_c \approx 1$ mol %, $w_c \approx 3.9$ wt %; F26C: $n_c \approx 2.3$ mol %, $w_c \approx 23.4$ wt %) do not have a substantial influence on the damping function. It is not surprising that the comonomer content does not influence the damping function, when considering the very small influence of short-chain branches on the linear-viscoelastic behavior (see, e.g., their small influence on the η_{0-M_w} correlation).[27] As the molar mass distribution has a substantial influence on linear-viscoelastic properties, one would expect that also the damping function is influenced by that. However, this is not the case. An explanation might be that the time dependence of the moduli is influenced by the molar mass distribution but not their values relative to each other, i.e., their damping function.

Comparing the measured data with the prediction of the Doi–Edwards (DE) model and the modeling by the PSM model (thin lines), a clear deviation from the experimental values is obvious which is mainly reflected by the higher double-logarithmic slope of −2 of these models. The Doi–Edwards model fits the data fairly well for $\gamma_0 < 200\%$, while the PSM model predicts the higher deformations between 500 and 5000% to some degree.

The excellent fit of the damping function using eq 6 (broken thick line) was found for γ_c of 200% and a terminal double-logarithmic slope m of −1.46. The bending parameter b was 1.66.

Polypropylenes. The isotactic polypropylenes were chosen to cover quite a range of molar masses and polydispersities (cf. Table 2). The damping functions of these samples are shown in Figure 4. It is evident that no significant difference is found between the various samples. However, samples with a high viscosity such as PP-A could not be measured up to high strains. The maximum deformation measured for PP-A was 500%. In the range determined, the molar mass and its distribution do not influence the damping function. Similar results have been reported in the literature. Fulchiron et al.,[10] for example, found no influence of the molar mass and its distribution on $h(\gamma_0)$ for polypropylenes with polydispersities between 2.8 and 5.6.

The best fit of the damping functions using eq 6 was found to have a terminal slope of −1.56, a bending parameter b of 1.82, and a γ_c value of 175%. When comparing these data to those of the linear polyethylenes, it is evident that the slope is somewhat steeper and that γ_c is lower (see Table 3).

Table 3. Fit Parameters of the Damping Functions of the Linear Samples

	lin. PP	lin. PE
m	−1.56	−1.46
b	1.82	1.67
γ_c (%)	175	202

The differences may be explained by the different entanglement structure. The entanglement molar mass M_e is reported to be around 830 g/mol for PE and around 5500 g/mol for isotactic PP.[46] This means that the number of entanglements at the same molar mass is higher for PE by a factor of about 6 than for PP. Thus, PP may be easier to disentangle than PE because of its less dense entanglement network. Therefore, a smaller deformation already causes a nonlinear behavior, which is a result of the partial disentanglement.

Damping Functions of Long-Chain Branched Samples. *Polyethylene.* The damping functions of the long-chain branched PE samples are shown in Figure 5. While the damping functions of the LCB-PE is essentially identical to the linear samples for $\gamma_0 < 100\%$, clear differences become obvious at larger strains, namely, a weaker strain dependence of the long-chain branched samples.

From Figure 5, it is evident that the samples LCB-mHDPE D4 and B5, which appear to be linear in SEC-MALLS measurements but slightly branched in linear rheological experiments,[47] show a rather small deviation from the curve of the linear products, while the three samples with the higher degree of branching (cf. Table 1) deviate more strongly. The LDPE fits very well with the higher branched LCB-mPE samples. This finding is somewhat surprising, as the LDPE possesses a totally different branching architecture.

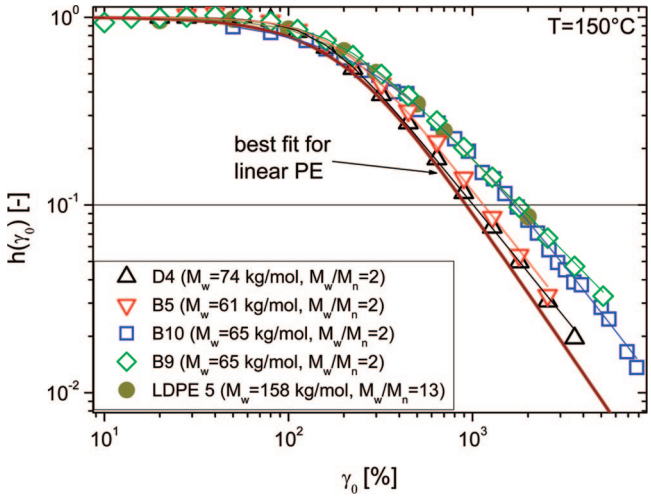

Figure 5. Damping functions of the long-chain branched polyethylenes.

The differences become more obvious when normalizing the damping functions of the LCB-PE with the damping function of linear PE (Figure 6). This plot shows that the damping functions of the LCB-PEs have similar γ_c values. For larger deformations, they reach a constant slope, which is smaller than that of the linear PE, resulting in higher normalized values (cf. Figure 6). It is clearly seen from the normalized plot that the differences between the linear and the weakly branched samples are small.

The fit parameters of the damping functions of the long-chain branched samples are summarized in Table 4.

Polypropylene. The damping functions of the long-chain branched polypropylenes in comparison to the linear base material PP-B are plotted in Figure 7. The LCB-PP show a distinct deviation toward higher values of $h(\gamma_0)$ in the nonlinear

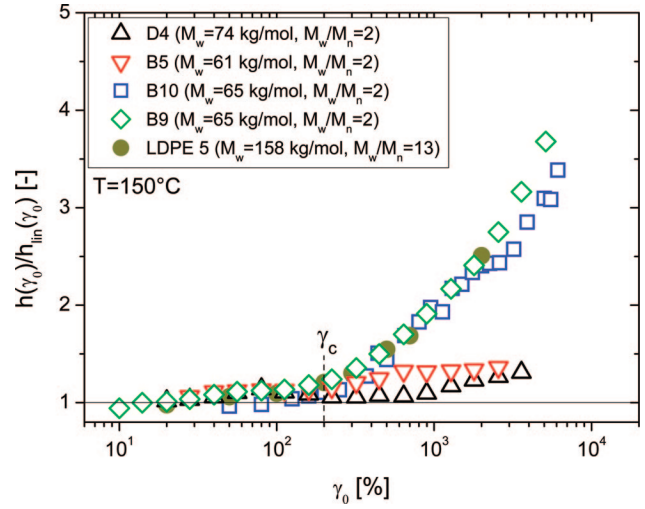

Figure 6. Normalized damping functions of the long-chain branched polyethylenes.

Table 4. Fit Parameters of the Damping Functions of the Long-Chain Branched Samples

	LCB	m	b	γ_c (%)	$\gamma_0(h = 0.1)$ (%)
D4	very low[a]	−1.21	2.74	150	1016
B5	low[a]	−1.25	2.35	184	1149
B10	low[a]	−1.25	1.22	294	1727
B9	medium	−1.05	2.11	195	1737
LDPE 5	high	−1.03	1.87	190	1750
PP-B2	very low[a]	−1.56	1.82	175	900
PP-B10	low	−1.23	2.31	129	1084
PP-B20	low	−1.16	1.81	150	1472
PP-B60	medium	−1.32	1.37	363	2672
PP-B100	high	−1.46	1.15	664	3855

[a] No branches were detected by SEC-MALLS for these samples, but rheological measurements in the linear-viscoelastic regime and the temperature dependence clearly indicate that the samples are long-chain branched.[28,30,37]

regime compared to the linear material. The differences with respect to the linear PP increase with higher irradiation doses, i.e., with higher degrees of long-chain branching. For the sample PP-B2, which behaves like a linear sample in SEC-MALLS and only shows a very slight indication of long-chain branches in rheological experiments, no significant deviation from the linear standard PP-B is observed. The damping functions of the samples PP-B10 and PP-B20 come to lie on the linear standard up to deformations of 200%, which are already distinctly in the nonlinear regime ($h(\gamma_0 = 200\%) \approx 0.5$). The samples PP-60 and PP-100, which have the highest degree of branching, show a growing linear regime but an even more substantial deviation from the linear standard (cf. Figures 7 and 8).

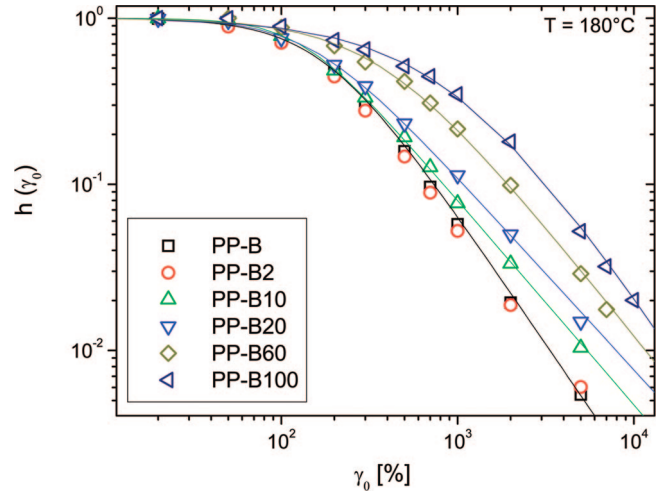

Figure 7. Damping functions of the long-chain branched polypropylenes.

The fit of the damping function using eq 6 (full lines) works well for PP-B, PP-B2, and PP-B10, while, for PP-B20, PP-B60, and PP-B100, the fit becomes more and more unsuitable to describe the damping function sufficiently well.

Comparison between Long-Chain Branched Polyethylene and Polypropylene. The damping functions of the linear PE and PP samples are quite different from each other. To compare the different damping functions, the deformation γ_0 at which the damping function reaches a value of 0.1 was chosen.[48]

For the PP, a significant increase of $\gamma_0(h = 0.1)$ is found with irradiation (Figure 8). For PE, the increase is not so pronounced. The reason for these differences is not known, but the assump-

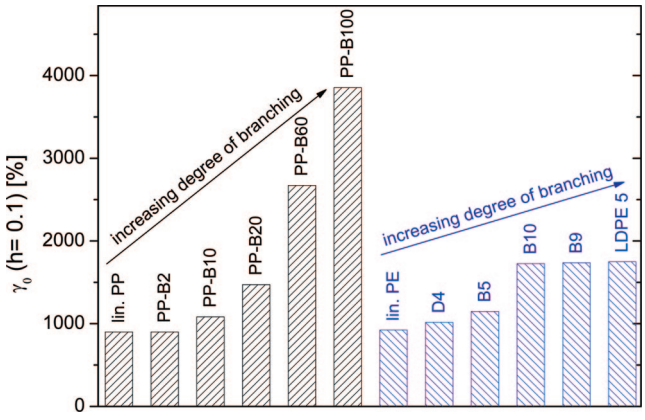

Figure 8. $\gamma_0(h = 0.1)$ for the different samples.

tion is obvious that it is a consequence of the different branching topography.

Interpretation of the Parameters of the Proposed Model. The proposed numerical description of the damping function contains three parameters whose relation to the molecular structure is explained in the following:

(1) The critical deformation γ_c is the onset of the nonlinear behavior. This deformation can be interpreted as the start of the disentanglement of the chains, which corresponds to the onset of chain retraction in terms of the DE-tube model.[21,45]

(2) The slope of the nonlinear regime m describes the sensitivity of the entanglement network toward disentanglement. While the results in the literature agree that the slope does not depend on the molar mass, it varies slightly with the *MMD*, but this dependence was only found in the literature to be significant for $M_w/M_n < 2$; i.e., it should not be of importance for the samples of broader distribution in this article.[9,21,45] For polydisperse systems[9] and topographies with two or more branch points per molecule, i.e., molecules with inner segments, a distinctly weaker strain dependence is observed.[13,18] Thus, the slope can be taken as an indicator of the existence of inner segments in the sample, which cannot disentangle as easily as outer segments.

(3) The width of the transition is given by the parameter b. This quantity is assumed to give an insight into the composition of the polymer. A sample, containing sizable amounts of, for example, combs, pom-poms, or trees and linear molecules is expected to show a broad transition zone of the damping function, while polymers with homogeneous topographies are expected to have a relatively narrow transition zone.

The parameters found for the long-chain branched samples investigated can thus be interpreted as follows: The incorporation of sparse long-chain branches into mPE leads to the formation of long-armed stars, which, although at very small concentrations, effects a distinct decrease in slope, while the onset of the nonlinear regime γ_c stays approximately the same. This can be understood by the fact that all the samples still contain significant amounts of linear chains.

For the LCB-PPs, a clear decrease of the slope m with increasing irradiation dose is obvious, while no such clear correlation can be found for γ_c and b, as they remain unchanged within the error of the fit procedure. This correlates with the very small degree of long-chain branching induced by irradiation doses below 20 kGy. PP-B100 and to a smaller extent also PP-B60 contain highly branched molecules as well as linear ones as determined from SEC-MALLS. The consequence of the relatively pronounced degree of branching is that the slope of the damping function of these samples is significantly smaller than that for all the other samples.

In comparison with the earlier models (DE, PSM), the new description has two distinct advantages. The first is that it offers a broader variety of shapes to be adapted, which allows a more precise description of the experimental data. This is achieved by decoupling the transition width parameter and the slope in the terminal regime, which is physically reasonable, as the position of the onset of nonlinearity is not connected to its width. Also, the new analytical description provides a more intuitive approach toward the meaning of the parameters "α" or "a" for the PSM and DE model (eq 3), as they are linked to γ_c for the proposed model (eq 6). The meaning of γ_c becomes immediately evident, while the same is not true for "α" or "a" in the PSM or DE model, respectively.

Conclusions

The damping functions of five linear and short-chain branched PEs and four linear PPs, varying in molar mass M_w, molar mass distribution, and degree of short-chain branching in the case of PE, were measured. The damping functions are independent of the molar mass and molar mass distribution in the range investigated. It was found that the type and content of comonomers do not influence the damping function, but linear polyethylene has a weaker strain dependence than linear polypropylene.

The long-chain branched samples show distinctly different damping functions. A higher degree of branching leads to a weaker dependence of the damping function on the deformation γ_0. Similar results were previously obtained on comb-polystyrenes.[6]

The long-chain branched polyethylenes (LCB-mPE and LDPE) show a decrease of the strain sensitivity, i.e., a lower slope at high γ_0 in comparison to linear samples. This effect increases with LCB concentration but seems to reach a saturation at already relatively low degrees of long-chain branching.

For the LCB-PPs, also a decrease of the strain sensitivity compared to the linear products was found, but compared to LCB-PE, this decrease is stronger and no saturation was reached. The increase of the irradiation dose leads to a decrease of the strain dependence of the relaxation modulus in comparison to the linear standards. This behavior can be interpreted assuming more highly branched structures, i.e., molecules with more than one branch point, as stars have almost the same damping function as linear chains.[14–16] The conclusion is, therefore, that a low degree of irradiation leads to the formation of very sparse stars with negligible amounts of more highly branched molecules, whose content increases with irradiation dose. This conclusion is in agreement with the straightforward picture on the reaction mechanism.

In the case of PP, the nonlinearity becomes distinctly weaker with increasing irradiation, i.e., growing branching efficiency. For the polyethylenes, the influence of the growing branching efficiency is less pronounced. Although the LDPE investigated does exhibit the highest degree of long-chain branching, if measured by SEC-MALLS, its nonlinearity is very similar to the long-chain branched metallocene HDPEs of lower branching density. Of course, the branching architectures are different. These comparisons clearly demonstrate that the deformation processes taking place in the melts of long-chain branched polyolefins are rather complex and far from being understood.

It was possible to describe the damping functions very well with a function using three parameters related to the slope at high strains, a critical strain γ_c for the deviation from the linear behavior, and a parameter describing the width of transition b from the constant to the power law function. With the exception of PP-B60 and PP-B100, the accuracy of the new analytical description was excellent.

The overall capability of the new model is significantly better than that of the DE and PSM damping functions. From a fundamental point of view, it is not understandable why the width of the transition and its starting point should be coupled as was done in the Soskey−Winter formula. The new numerical description proposed separates these two factors.

Moreover, it is possible to analytically conduct the correction for the non-Newtonian flow behavior, which is necessary because of the nonhomogeneous deformation field in parallel-plate geometries, by using the analytical description of this paper. Although splines could also be used for the determination of the local slope, the new model provides a more stable solution against problems related to experimental scatter, which can have a significant effect on the derivative (cf. eq 8). In the numerical description proposed, the coefficients have a physical meaning and allow conclusions with respect to the molecular structure of the materials investigated, which cannot be obtained by a spline.

Acknowledgment. The authors would like to thank the German Research Foundation (Deutsche Forschungsgemeinschaft) for financial support by the grants MU 1336-7 and MU 1336-9. The contributions of Dr. C. Piel and Prof. Dr. W. Kaminsky (University Hamburg) regarding the synthesis of many of the linear and long-chain branched polyethylenes. those of Dr. B. Krause, Dr. U. Lappan, and Prof. Dr. K. Lunkwitz (Leibniz-Institute of Polymer Research, Dresden) regarding the electron-beam-irradiated polypropylenes, and those of Dr. J. Kaschta and I. Herzer (University Erlangen-Nürnberg) for some SEC-MALLS measurements are gratefully acknowledged. Additional thanks go to S. Schuberth and A. Petzoldt (University Erlangen-Nürnberg), Dr. Salvatore Coppola (Polimeri Europa), Dr. Sunil Dhole (Université Catholique de Louvain), and Prof. Dr. M. H. Wagner (Technical University Berlin) for discussions and to Dr. Claus Gabriel (BASF AG) for providing the ZN-HDPE.

References and Notes

(1) Wagner, M. H.; Laun, H. M. *Rheol. Acta* **1978**, *17*, 138–148.
(2) Papanastasiou, A.; Scriven, L.; Macosko, C. *J. Rheol.* **1983**, *27* (4), 387–410.
(3) Soskey, P.; Winter, H. *J. Rheol.* **1984**, *28* (5), 625–645.
(4) Archer, L. A. *J. Rheol.* **1999**, *43* (6), 1555–1571.
(5) Larson, R. G. *J. Rheol.* **1985**, *29* (6), 823–831.
(6) Hepperle, J.; Münstedt, H. *Rheol. Acta* **2006**, *45* (5), 717–727.
(7) Urakawa, O.; Takahashi, M.; Masuda, T.; Ebrahimi, N. G. *Macromolecules* **1995**, *28* (21), 7196–7201.
(8) Osaki, K.; Takatori, E.; Kurata, M. *Macromolecules* **1987**, *20* (7), 1681–1687.
(9) Venerus, D. C.; Brown, E. F.; Burghardt, W. R. *Macromolecules* **1998**, *31* (26), 9206–9212.
(10) Fulchiron, R.; Verney, V.; Marin, G. *J. Non-Newtonian Fluid Mech.* **1993**, *48*, 49–68.
(11) Leblans, P. J. R.; Sampers, J.; Booij, H. C. *Rheol. Acta* **1985**, *24*, 152.
(12) Osaki, K.; Kurata, M. *Macromolecules* **1980**, *13* (3), 671.
(13) Archer, L. A.; Varshney, S. K. *Macromolecules* **1998**, *31* (18), 6348–6355.
(14) Vrentas, C. M.; Graessley, W. W. *J. Rheol.* **1982**, *26* (4), 359–371.
(15) Osaki, K.; Takatori, E.; Kurata, M.; Watanabe, H.; Yoshida, H.; Kotaka, T. *Macromolecules* **1990**, *23* (20), 4392–4396.
(16) Fetters, L. J.; Kiss, A. D.; Peareon, D. S.; Quack, G. F.; Vitus, F. J. *Macromolecules* **1993**, *26* (4), 647654
(17) Archer, L. A.; Juliani, *Macromolecules* **2004**, *37*, 1076–1088.
(18) Kirkwood, K. M.; Kapnistos, M.; Hadjichristidis, N.; Vlassopoulos, D.; Leal, G. *The nonlinear rheology of entangled linear comb polymer solutions*, The Society of Rheology 79th Annual Meeting, Salt Lake City, UT, 2007.
(19) Larson, R. G. *J. Rheol.* **1984**, *28* (5), 545.
(20) Kasehagen, L. J.; Macosko, C. W. *J. Rheol.* **1998**, *42*, 1303–1550.
(21) Doi, M.; Edwards, S. F. *The Theory of Polymer Dynamics*; Oxford-Press: Oxford, U.K., 1986.
(22) Equation 3 is not the formula derived from the DE model but a very good approximation.
(23) Larson, R. G. *Constitutive Equations for Polymer Melts and Solutions*; Butterworths: Boston, MA, 1998.
(24) The exact form of this equation given by Soskey and Winter[3] is $h_s(\gamma_0) = 1/(1 + \alpha \cdot \gamma_0^b)$, which is equivalent to eq 3. Equation 3 was published in that form by Papanastasiou et al.[2]
(25) Wagner, M. H.; Demarmels, A. *J. Rheol.* **1990**, *34* (6), 943–958.
(26) Laun, H. M. *Prog. Colloid Polym. Sci.* **1987**, *75*, 111–139.
(27) Stadler, F. J.; Münstedt, H. *J. Rheol.*, in press (DOI: 10.1122/1.2892039).
(28) Stadler, F. J.; Kaschta, J.; Münstedt, H. *Macromolecules* **2008**, *41* (4), 1328–1333.
(29) Stadler, F. J.; Piel, C.; Kaschta, J.; Rulhoff, S.; Kaminsky, W.; Münstedt, H. *Rheol. Acta* **2006**, *45* (5), 755–764.
(30) Piel, C.; Stadler, F. J.; Kaschta, J.; Rulhoff, S.; Münstedt, H.; Kaminsky, W. *Macromol. Chem. Phys.* **2006**, *207* (1), 26–38.
(31) Stadler, F. J.; Piel, C.; Klimke, K.; Kaschta, J.; Parkinson, M.; Wilhelm, M.; Kaminsky, W.; Münstedt, H. *Macromolecules* **2006**, *39* (4), 1474–1482.
(32) Stadler, F. J.; Piel, C.; Kaminsky, W.; Münstedt, H. *Macromol. Symp.* **2006**, *236* (1), 209–218.
(33) Stadler, F. J.; Gabriel, C.; Münstedt, H. *Macromol. Chem. Phys.* **2007**, *208* (22), 2449–2454.
(34) Gabriel, C.; Münstedt, H. *Rheol. Acta* **2002**, *41* (3), 232–244.
(35) Gabriel, C.; Münstedt, H. *J. Rheol.* **2003**, *47* (3), 619–630.
(36) Stadler, F. J.; Münstedt, H. *Journal Non-Newtonian Fluid Mech.*, in press (DOI: 10.1016/j.jnnfm.2008.01.010).
(37) Auhl, D. *Molekulare Struktur und rheologische Eigenschaften von strahlenmodifizierten Polypropylen*; Friedrich-Alexander Universität Erlangen-Nürnberg, Erlangen, Germany, 2006.
(38) Auhl, D.; Stange, J.; Münstedt, H.; Krause, B.; Voigt, D.; Lederer, A.; Lappan, U.; Lunkwitz, K. *Macromolecules* **2004**, *37* (25), 9465–9472.
(39) Krause, B.; Voigt, D.; Lederer, A.; Auhl, D.; Münstedt, H. *J. Chromatogr., A* **2004**, *1056* (1–2), 217–222.
(40) Kaminsky, W.; Piel, C.; Scharlach, K. *Macromol. Symp.* **2005**, *226* (1), 25–34.
(41) Stadler, F. J. *Molecular Structure and Rheological Properties of Linear and Long-Chain Branched Ethene-/α-Olefin Copolymers*; Sierke-Verlag: Göttingen, Germany, 2007 (ISBN: 978-3-940333-24-7).
(42) Carreau, P. J. *Trans. Soc. Rheol.* **1972**, *16* (1), 99–127.
(43) Yasuda, K.; Armstrong, R. C.; Cohen, R. E. *Rheol. Acta* **1981**, *20*, 163–178.
(44) According to Larson and Dealy,[45] eq 3 is only an approximation of the real more complicated damping function of the DE model, and therefore, no direct physical meaning of α and β is given.
(45) Dealy, J.; Larson, R. G. *Structure and Rheology of Molten Polymers - From Structure to Flow Behavior and Back Again*; Hanser: Munich, 2006.
(46) Fetters, L.; Lohse, D.; Graessley, W. *Polymer* **1999**, *37* (10), 1023–1033.
(47) The zero shear-rate viscosity η_0 is distinctly above the value expected from the molar mass M_w according to the correlation $\eta_0 \sim M_w^{3.6}$ (see Stadler et al.[29,31] for more details).
(48) This value was chosen to be as low as possible to find pronounced differences but high enough that all LCB samples can be compared.

MA0717587